An Ultra-small Thermosenstive Nanocomposite with Mo_{154}-Core as Comprehensive Platform for NIR-Triggered Photothermal-Chemotherapy

Simin Zhang,[†] *Haobin Chen,*[‡] *Guohua Zhang,*[†] *Xueping Kong,*[†] *Shengyan Yin,*[‡] *Bao Li*[†] *and Lixin Wu**,[†]

[†]State Key Laboratory of Supramolecular Structure and Materials, Jilin University, Changchun, 130012, China.

[‡]State Key Laboratory on Integrated Optoelectronics, College of Electronic Science and Engineering, Jilin University, Changchun, 130012, China.

Supporting Information

Table of Contents

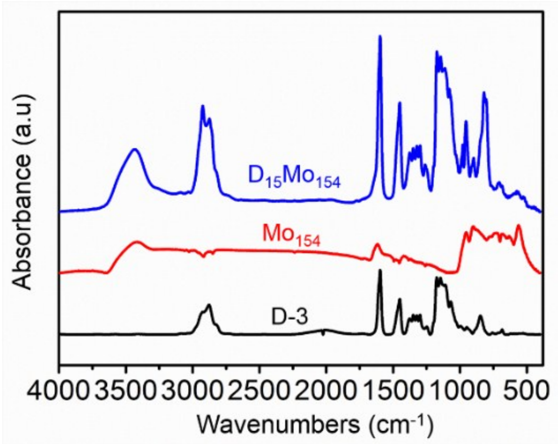

Figure S1. IR spectra of pure $D_{15}Mo_{154}$, Mo_{154}, and D-3 in KBr pellets.

Table S1. The assignments of infrared spectra of $D_{15}Mo_{154}$ in solid state.

D-3/cm^{-1}	$D_{15}Mo_{154}$ /cm^{-1}	Assignment	D-3/cm^{-1}	$D_{15}Mo_{154}$ /cm^{-1}	Assignment
		O–H asym. str.	1248	1250	CH_2 twisting
2933	2933	CH_3 asym. str.	1173	1172	=C–O–C asym. str.
2823	2824	CH_2 sym. str.	1116	1114	C–O–C stretching
1597	1597	C=C frame str.	1068	1068	=C–O–C asym. str.
1454	1452	CH_2 scissoring		978, 914	v(Mo=O)
1385	1380	CH_3 scissoring	844	847	CH str.
1350	1352	CH_2 wagging		750,630,559	
1325	1323	CH_2 wagging	758		CH_2 rocking
1297	1297	CH_2 twisting			

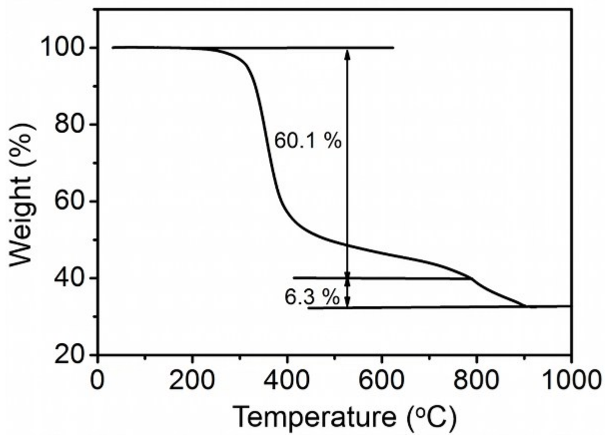

Figure S3. TGA curve of $D_{15}Mo_{154}$.

Table S2. The summary of elemental analysis for the prepared complex.[a]

		C	H	N	Mo
$D_{15}Mo_{154}$	Calcd. (%)	35.56	4.82	0.38	27.00
	Found (%)	35.28	4.88	0.35	26.57

[a] The elemental analytical results of C, H and N were obtained from organic elemental analysis, and the elemental analysis of Mo was performed on inductive coupled plasma emission spectrometer.

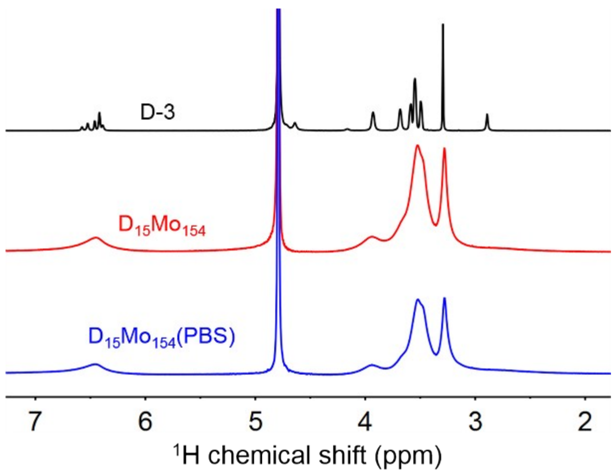

Figure S4. ^{1}H NMR spectra of D-3, and $D_{15}Mo_{154}$ in D_2O solution without and with phosphate buffer (PBS).

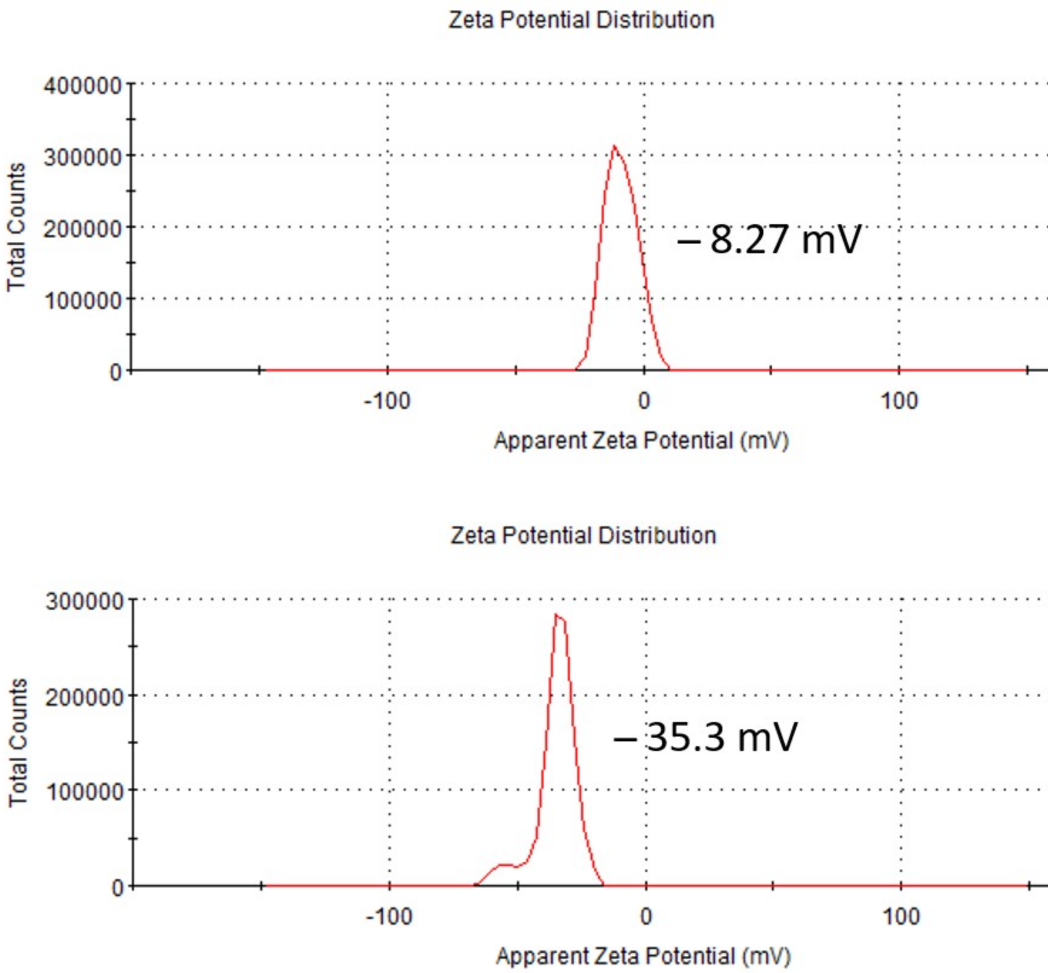

Figure S5. Zeta potential of (a) D-GdSiW-R complex and (b) pure $GdSiW_{11}$ in aqueous solution, where the concentration is fixed at 0.05 mM.

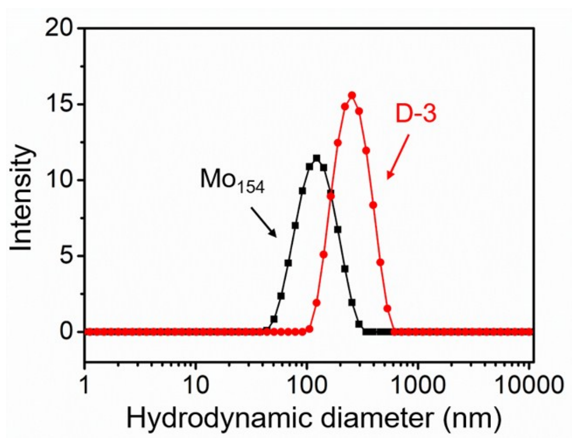

Figure S6. DLS curves of D-3 and Mo_{154} in aqueous solution, where the concentration of Mo_{154} is 0.03 mM and D-3 is 0.45 mM.

Calculation of photothermal conversion efficiency (η) of $D_{15}Mo_{154}$

Calculation of θ.

The θ is a dimensionless driving force temperature.

$$\theta = \frac{T - T_{Surr}}{T_{Max} - T_{Surr}} \tag{1}$$

where T is the solution temperature, T_{Surr} is ambient temperature of the surroundings, and T_{Max} is the equilibrium temperature.

Calculation of τ_s.

The τ_s is system heat-transfer time constant and it is estimated according to Figure S7b.

$$\tau_s = -\frac{\ln \theta}{t} \tag{2}$$

Calculation of hS.

The h is heat transfer coefficient, S is the surface area of the container.

$$hS = \frac{\sum_i m_i C_{p,i}}{\tau_s} \tag{3}$$

where m and Cp are the mass and heat capacity of water, respectively.

Calculation of η.

The η is the photothermal conversion efficiency of $D_{15}Mo_{154}$.

$$\eta = \frac{hS(T_{Max} - T_{Surr}) - Q_{dis}}{I(1 - 10^{-A_{808}})} \tag{4}$$

where, I is incident laser power, A_{808} is absorbance of $D_{15}Mo_{154}$ in a sample cell at wavelength 808 nm, Q_{dis} expresses heat dissipated from light absorbed by the container itself, and it is calculated independently using a container containing pure water.

In the present system, we get the plot of $-\ln\theta$ versus the time in Figure S7b, according to equation (1), in which T parameteres are estimated from Figure S7a. Therefore, τ_s is calculated to be:

$$\tau_s = -\frac{\ln\theta}{t} = 420.2073$$

$$hS = \frac{\sum_i m_i C_{p,i}}{\tau_s} = 0.01$$

Because $Q_{dis} = \frac{cm\Delta T}{t} = \frac{4.2 * 10^{-3} J/(kg \cdot °C) * 10^{-3} kg * (27°C - 24°C)}{300s} = 0.042\ J \cdot s^{-1}$

and $A_{808} = 1.3$, thus,

$$\eta = \frac{hS(T_{Max} - T_{Surr}) - Q_{dis}}{I(1 - 10^{-A_{808}})} = 30.9\ \%$$

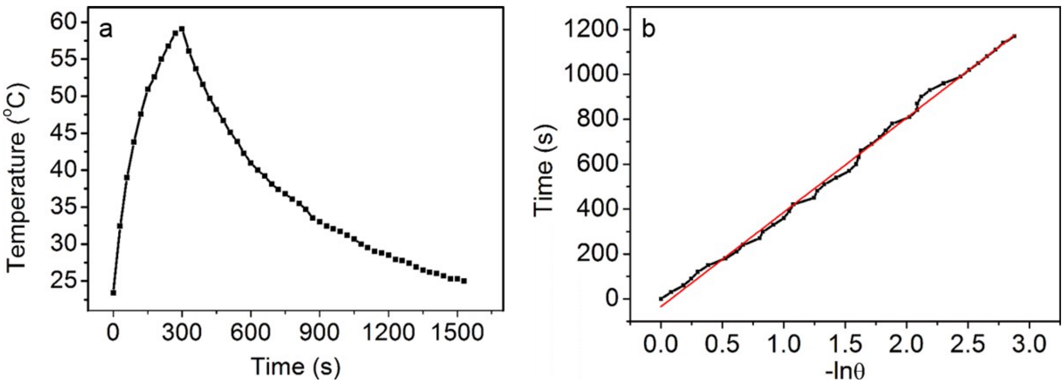

Figure S7. (a) The plot of temperature variation in $D_{15}Mo_{154}$ aqueous solution that encounters a 808 nm laser irradiation at a power density of 1 W/cm^2 for 300 s and then cooled to room temperature gradually under ambient environment; and (b) plot of time versus the $-\ln\theta$ obtained from the cooling period in Figure S7a, where the solution volume is 1 mL.

Table S3. The summary of loading capacity of DOX in $D_{15}Mo_{154}$.

Initial molar

ratio of $D_{15}Mo_{154}$:DOX	Initial mass of DOX (mg)	unreacted mass of DOX (mg)/Abs [a]	Loading capacity [b]
1:10	2.9	1.439/0.192	1:5

[a] The free (unloaded) DOX is taken from outside the dialysis bag and calculated from the following work plot of absorbance in UV-vis spectra versus the concentration of pure DOX·HCl in aqueous solution.

[b] The loading capacity is defined as molar ratio of $D_{15}Mo_{154}$ to DOX.

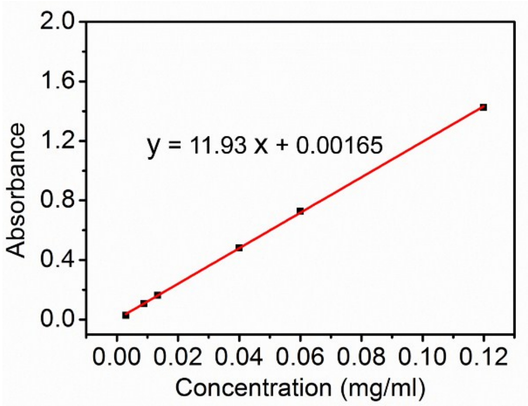

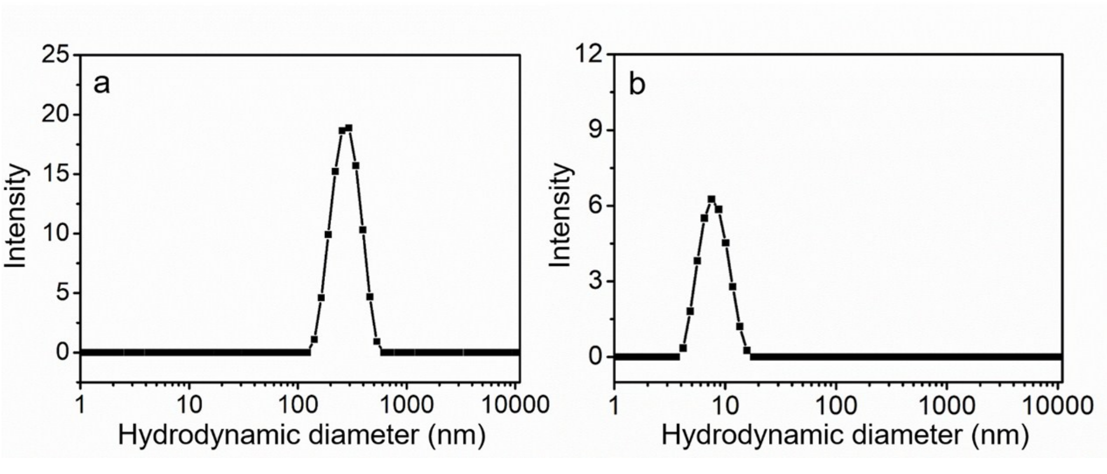

Figure S8. DLS curves of (a) DOX·HCl and (b) $D_{15}Mo_{154}$@DOX in aqueous solution.

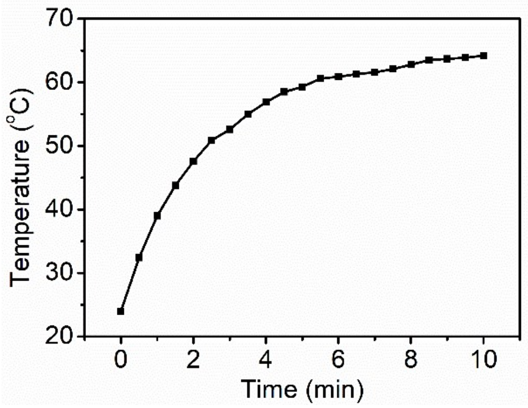

Figure S9. Photothermal heating curve of $D_{15}Mo_{154}$@DOX aqueous solution (0.05 mM) under exposure of 808 nm laser (power density of 1 W/cm^2) versus time.